PROCEEDINGS, 45th Workshop on Geothermal Reservoir Engineering
Stanford University, Stanford, California, February 10-12, 2020
SGP-TR-216

Exploring Hydraulic Fracture Stimulation Patterns in the FORGE Reservoir Using Multiple Stochastic DFN Realizations and Variable Stress Conditions

Aleta Finnila[1] and Robert Podgorney[2]

[1]Golder Associates Inc., 18300 Union Hill Road, Redmond, WA 98052

[2]Idaho National Laboratory, 1955 N. Fremont Ave, P.O. Box 1625, Idaho Falls, ID 83415

afinnila@golder.com

Keywords: FORGE, modeling and simulation, DFN, reservoir planning, stimulation, hydraulic fracturing.

ABSTRACT

Numerical simulations of hydraulic fracturing require a starting representation of the natural fractures present. The natural fractures in the FORGE reservoir are modeled as a Discrete Fracture Network (DFN). One DFN represents a single realization of a population that is only approximated through knowledge of its averaged properties. While each realization of the DFN created will share statistically equivalent properties, there will be local variations in individual fracture locations, sizes and orientations. In order to find representative (e.g., min, max, median, 95% percentile, etc.) DFN realizations that are most useful for refined numerical simulation work, one hundred realizations of the DFN are generated and stimulated using the FracMan code. This code simplifies some of the underlying physics to enable rapid simulation of very large networks and is used as a screening tool to identify representative average and end-member DFN realizations for use by other modelers in more detailed studies of stimulation development.

Due to the range of possible stress conditions at the FORGE site, eighteen different stress conditions were applied during the hydraulic fracturing simulations. These included combinations of three principal horizontal stress orientations, three maximum horizontal stress gradient magnitudes, and two different minimum horizontal stress gradient magnitudes. Each stress condition was used for thirty of the DFN realizations while the most likely stress condition was applied to all one hundred DFN realizations. Simulation extents including both inflated fractures and hydrosheared fractures were recorded in the East-West, North-South and vertical directions and patterns analyzed. Patterns in the stimulation bounding box anisotropy with respect to differing stress conditions are highlighted. Stimulation extents in the East-West direction are uniformly smaller than those in the North-South and vertical directions.

1. INTRODUCTION

Hydraulic stimulation plans for a new well at the Frontier Observatory for Research in Geothermal Energy (FORGE) site in Milford, Utah, require predictions of the reservoir response to various injection scenarios. What is the extent of stimulation? Will the stimulated zone exceed the property boundaries (Figure 1)? What is the expected microseismic response? These questions and many others can be approached using various numerical modeling techniques; however, all of the techniques require accurate estimates of the rock properties, natural fracture network and the local stress conditions. This paper shows the work performed to get the most useful representations of the natural fracture network for use by the FORGE modeling team considering the current uncertainty in the stress conditions at the site.

The natural fractures present in the reservoir are modeled as a Discrete Fracture Network (DFN). While the location and orientation of a subset of the fracture population are known from image log data from the exiting vertical pilot well, 58-32, fractures further away from the existing well are modeled using stochastically generated fractures. These stochastic fractures have property distributions which are consistent with the measured fracture parameters for size, orientation and intensity; however, different realizations of this stochastic DFN will show varying local properties such as heterogeneity and connectivity. If a particular realization of a DFN is selected to represent the initial conditions for a numerical simulation, how confident can we be that the results would not be significantly changed if a different DFN realization was used? Can we ensure that the realization selected is “average”? Can we show how the results would be affected if some type of “end-member” DFN realization had been selected instead? These questions are complicated by the fact that an “average” DFN realization only has meaning in the context of how that realization is being affected by a simulation.

In the case of using the DFN for hydraulic fracturing, it is the interaction between the orientations of the natural fractures and the stress conditions that control the response to stimulation. How an individual, planar fracture responds to stimulation caused by increased pore pressure is a function of both the fracture orientation and the local stress field. While the vertical stress gradient is well determined, there is currently a range of possible values for the direction and magnitude of the principal horizontal stress and the magnitude of the minimum horizontal stress. Therefore, there is a question both of how much variation in the results of a numerical simulation are due to the choice of a particular DFN realization, and how much variation is expected due to the uncertainty in the stress state. This paper addresses both questions by performing over six hundred simplified hydraulic fracture simulations on one hundred DFN realizations using a matrix of eighteen different stress conditions. The hydraulic stimulation parameters are kept constant using a two-hour stimulation at a pumping rate of 50 kg/s.

Thirty DFN realizations are created and then stimulated using Golder Associates’ FracMan DFN code (Golder, 2020) using each of the potential stress conditions. One hundred DFN realizations are used for the most likely stress condition. The extent of both inflated

fractures and hydrosheared fractures in the vertical, East-West, and North-South directions is measured. Given the reduced physics included in the FracMan hydraulic simulations, the absolute values for the extent distances are not expected to be accurate. Therefore, the distances are presented as normalized values in box plots where median, quartile, and extreme values are easily visualized. The patterns displayed by the relative extent distances, however, including the ranking of how the realizations respond to the different stress conditions are expected to be correct. Of particular interest is how much anisotropy is expressed during the stimulations. Box plots of the ratios comparing the three stimulation distances for each simulation are presented to investigate the geometry of each DFN realization/stress-state pairing.

The end goal of this work is to select a small number of DFN realizations to use in the more time-consuming numerical modeling methods that will be used for detailed studies of stimulation development. These selected realizations will show average, minimum and maximum responses to hydraulic stimulation, given a choice for stress conditions.

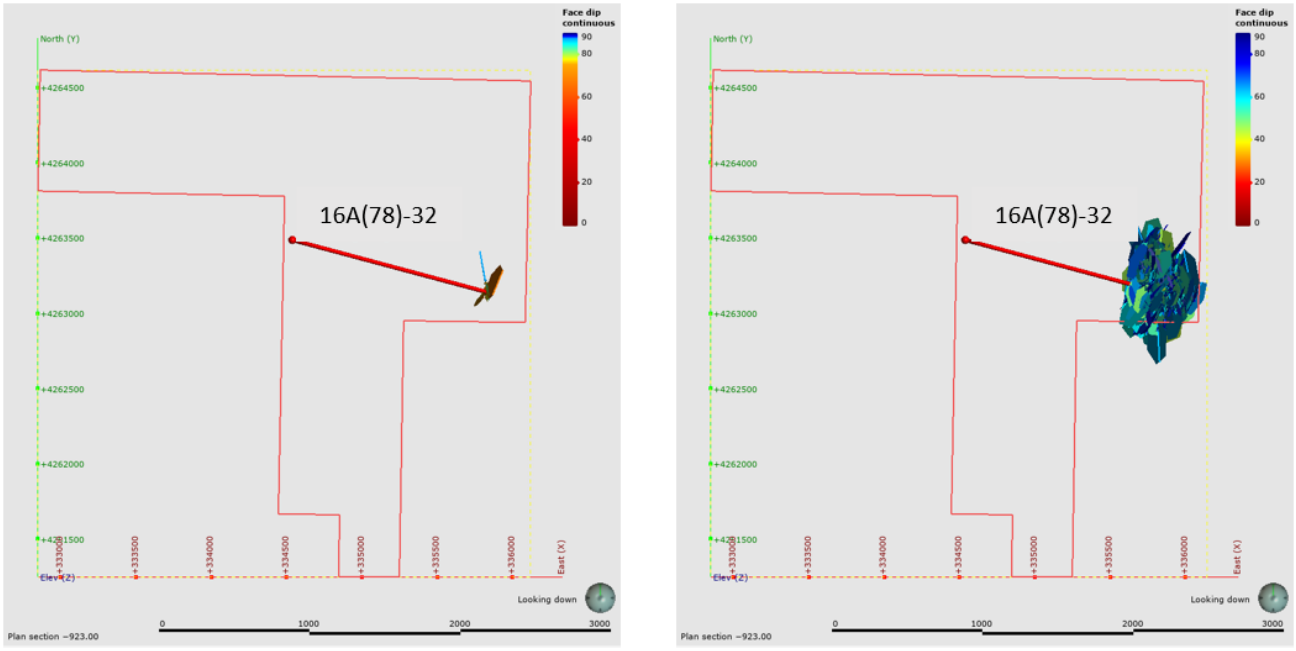

Figure 1: Top down view of inflated (left) and hydrosheared (right) fractures from a hydraulic fracture simulation at the toe of the proposed injection well, 16A(78)-32. The FORGE property boundaries are shown in red.

2. MODEL SETUP

2.1 Model Region

The FORGE site is located west of the Roosevelt Hot Springs near the town of Milford, Utah (Figure 2). The proposed new injection well, 16A(78)-32, is expected to descend vertically to a depth of approximately 1800 m and then extend laterally at a 105° azimuth and final 25º dip to a MD of approximately 3500 m and a maximum vertical depth of approximately 2670 m (Figure 3). There is approximately 1500 m of basin fill at the well head, and less than that above the simulation region with the targeted reservoir region fully enclosed in granitoid basement. The last 60 m of the well will be open hole. This open hole section is used in the hydraulic stimulation simulations included in this paper. The DFN realizations were generated in a 1200 m box centered at the injection site while the hydraulic stimulation simulations were restricted to an 800 m box having the same center. While 2 million fractures were generated in the 1200 m box, only 600 thousand were located in the smaller 800 m region. Restricting the number of fractures in this way decreased the running time for each simulation from 2 hours to 10 minutes. Since the largest stimulated extent measured in all the simulations was less than 700 m, edge effects are not expected to be an issue. Generating the fractures in a larger volume has the benefit of ensuring their availability for future simulation work requiring larger modeling regions while still being pre-screened for their stimulation behavior in the open-hole section of the well.

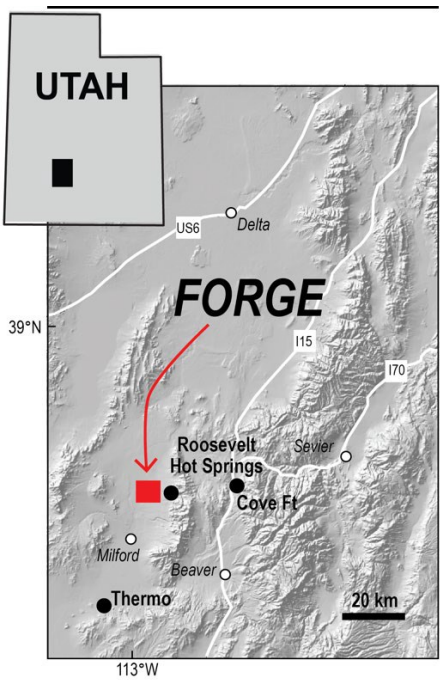

Figure 2: Location of the FORGE site (Moore et al., 2019).

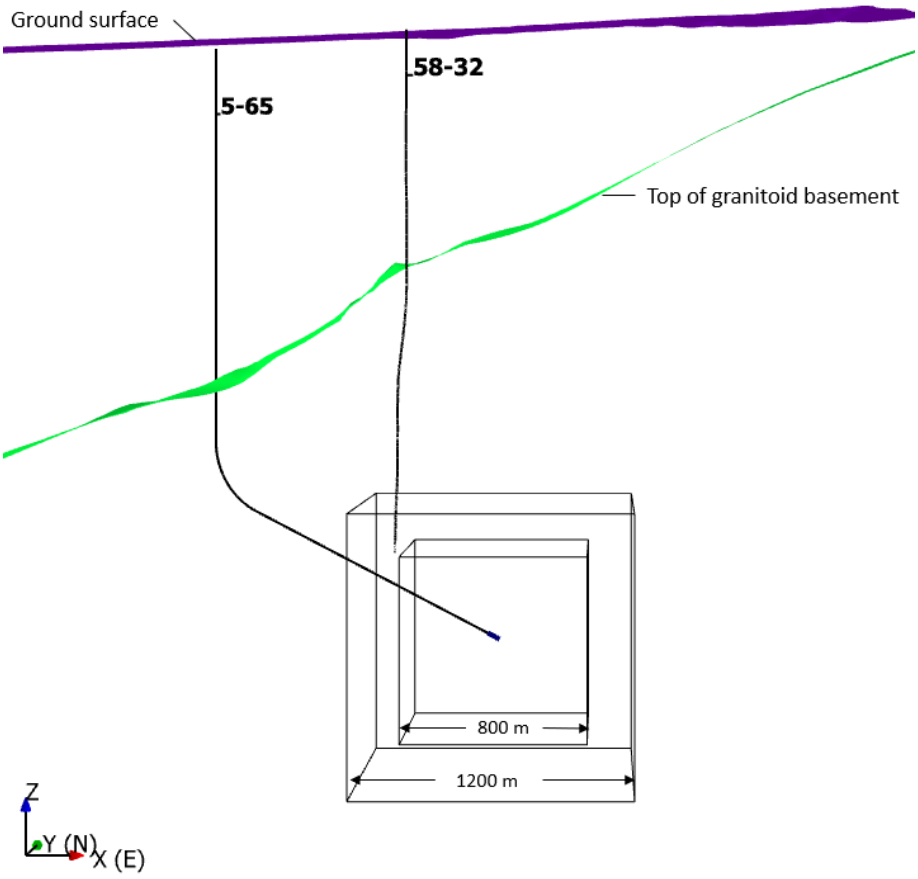

Figure 3: Modeling region.

2.2 DFN

The DFN was based on the FORGE Reference DFN described in Finnila et al. (2019), adjusted to use a power law fracture size distribution. Fractures were generated using the FracMan code. Input parameters for the creation of the DFN are shown in Table 1. One hundred DFN realizations were created using different starting seeds for the random number generator. These seed values were saved so that the generated DFN realization could be re-generated if needed as each realization was deleted after being stimulated in preparation for the next realization. It is faster to regenerate a particular DFN realization than it is to write and load a saved copy from disk.

Table 1: Fracture parameters used to generate the DFN realizations in FracMan.

Intensity P_{32} [1/m]	1.3
Orientation	based on Terzaghi-weighted FMI log from 58-32 with a Fisher concentration parameter of 50
Size Distribution	Power Law (Pareto with X_{min}=1 and α=2.6)
Min Size (Equivalent Radius) [m]	10
Max Size (Equivalent Radius) [m]	150
Shape	regular polygon with 6 sides
Aperture [mm]	0.607*EquivalentRadius[m]^0.5
Permeability [m^2]	$1.66x10^{-15}$*Aperture[mm]^1.5
Compressibility [1/kPa]	$7.14x10^{-6}$

2.3 Stress State

The FORGE site is located in a normal stress regime. The direction of S_{Hmax} was determined from the orientation of tensile fractures identified in the image log for 58-32. As seen in Figure 4, there was a wide spread of orientations measured so there is significant uncertainty. The best estimate of N25E +/- 15 degrees was considered adequate to capture the range of evidence (N10E, N25E, N40E). The work by Xing et al. (2020) was used to determine the recommended values and the minimum value for S_{hmin}. The value for S_{Hmax} is much more uncertain. A minimum value equal to the recommended value of S_{hmin}, and a maximum value equal to the recommended and relatively well-constrained vertical stress were used in order to look at the widest range possible while still representing a normal stress state. The pore pressure and vertical stress gradients are well known and kept constant for all of the simulations. The matrix of stress conditions is shown in Table 2 with the two fixed stress conditions shown in green and the five varying stress conditions shown in gold.

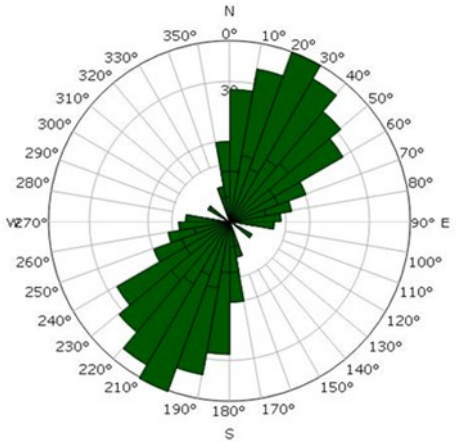

Figure 4: Orientation of S_{Hmax} from induced tensile fractures identified in 58-32 (Simmons et al., 2018).

Table 2: Stress gradients and orientations used to create the various stress conditions used for hydraulic fracturing. The pore pressure and vertical stress gradients were kept constant (green background) while all the permutations associated with the range of S_{Hmax}, S_{hmin} and the orientation of S_{Hmax} were tested (gold background). In all, there were 18 stress gradient/orientation combinations examined.

	Recommended	Minimum	Maximum
Pore Pressure [MPa/km]	9.7	N/A	N/A
Vertical Stress [MPa/km]	25.6	N/A	N/A
S_{Hmax} [MPa/km]	21.3	17.0	25.6
S_{hmin} [MPa/m]	17.0	13.8	N/A
Direction S_{Hmax}	N25E	N10E	N40E

2.4 Hydraulic Fracturing

The hydraulic fracturing simulations use the FracMan code which is based on the theory of critical stress analysis and involves solving a constitutive relation conserving the material mass within the fracture network (Dershowitz et al, 2011; Cottrell et al., 2013). An induced tensile fracture develops from the well having a normal parallel to the minimum stress direction. Intersecting natural fractures having a normal stress less than the fracture pore pressure also accept water. FracMan simulates the hydraulic fracturing by maintaining a volume balance between the pumped water and the expanded volume of the natural fractures and the developed hydraulic fracture. Input parameters are shown in Table 3.

Table 3: Hydraulic fracturing parameters used for FracMan simulations.

Pumping duration [hr]	2
Pumping rate [kg/s]	50
Delta pressure [MPa]	6.9
Flowback [%]	5
Minimum injection ratio to new hydraulic fracture [%]	10
Water density [kg/m3]	1000
Water viscosity [Pa s]	0.00089
Rock lithology	granitoid
Young's modulus [GPa]	55
Poisson's ratio	0.27
Frictional model	Mohr-Coulomb
Friction angle [deg]	36
Cohesion [MPa]	2
New tensile fracture location	best oriented with respect to the maximum horizontal stress
Bounding box	800 m region box
Element size [m]	10
Fracture set	full stochastic set in the 800 m box region
Fracture pressure mode	Secor and Pollard
Pore pressure slope with distance	0.5
Flow to fracture order	(transmissivity*orientation)/ (connection_level)
Maximum aperture for inflated fractures [mm]	5
Pressure decrease with distance from inflated fracture	linear
Reservoir pore pressure [MPa]	24.6
Hydroshear element size [m]	10
Hydroshear distance [m]	250

3. WORKFLOW

The workflow implemented was to generate one realization of the DFN using a known seed value for the random number generator and then run eighteen hydraulic fracture simulations on that realization with each run corresponding to a different potential stress condition. Seventy extra realizations were generated for the most likely stress condition (for a total of one hundred). Reports for each hydraulic fracture simulation were saved as text files for later analysis. Then the DFN realization was deleted and a new one generated for the next round of analyses. After the simulations were complete, the reports were aggregated and both detailed and summary spreadsheets were generated. The summary data includes the mean, standard deviation, median, min, max, and realization numbers for the average and extreme values for all of the measurements of interest: the extent of both inflated fractures and hydrosheared fractures in the vertical, East-West, and North-South directions.

Stimulation extents in the cardinal and vertical directions are reported for each simulation performed for all the stimulated fractures which includes both inflated and hydrosheared events (Figure 5). These two populations were investigated independently since the inflated fractures tend to be vertical while the hydrosheared fractures tend to be more inclined in this normal stress regime. These two populations are impacted differently by changing the initial stress state. Aspect ratios comparing the EW:NS, EW:Vertical, and NS:Vertical extents for both the inflated fractures and all the stimulated fractures are also shown to highlight the variation in stimulation anisotropy.

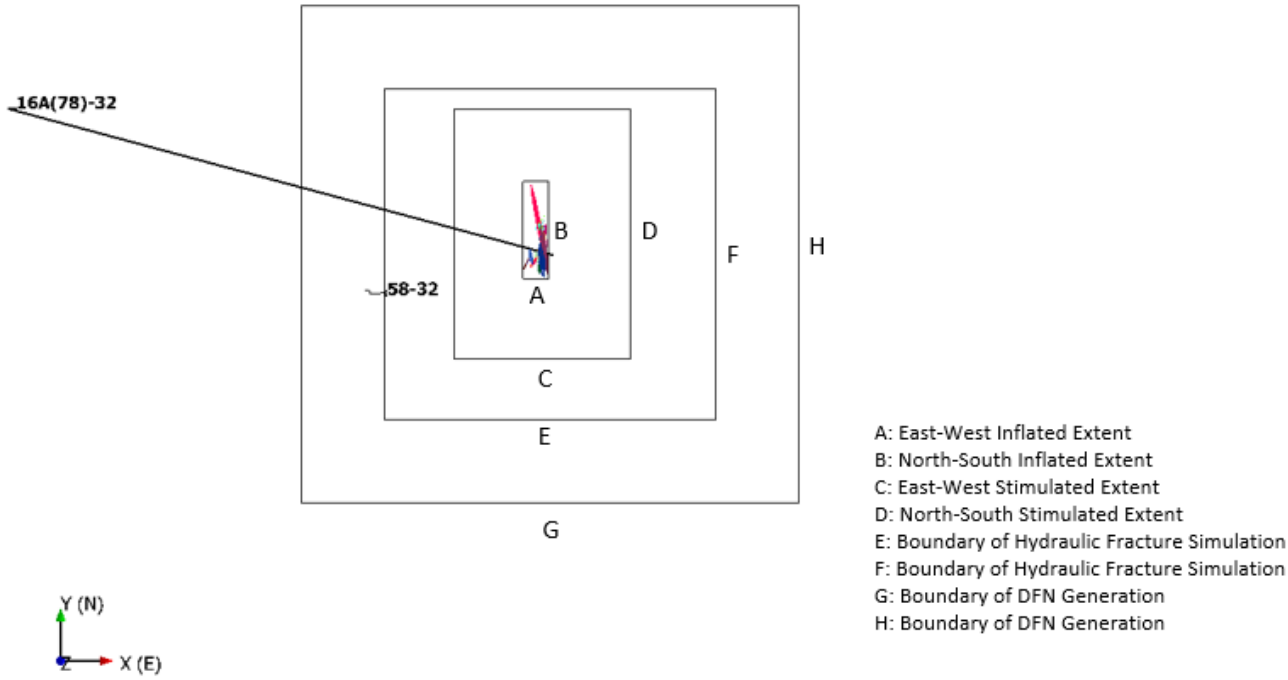

Figure 5: Top view of how inflation extents (A,B) and full stimulation extents (C,D) were measured for each hydraulic fracture simulation. The inflated fractures for one simulation are shown as colored planes connected to the proposed injection well, 16A(78)-32. The fractures that experience hydroshearing during the hydraulic fracture stimulation are not shown, but would be enclosed within the box with sides C and D. The existing vertical well, 58-32, is also shown for reference.

4. RESULTS

Given the estimation techniques utilized to achieve very rapid hydraulic fracturing simulation, the absolute stimulation distances produced in the simulations are not necessarily accurate, so they are normalized using the size of the bounding box (800 m for these runs) to emphasize that we are investigating the relative behavior of these fracture sets with this work, not the absolute values. Selected DFN realizations that are "average" or "extreme" can be identified and then used as inputs to full physics simulators in order to predict what the absolute stimulation extents might be. Therefore, the distances are presented as normalized values in both histograms and box plots where median, quartile, and extreme values are easily visualized. The patterns displayed by the relative extent distances, including the ranking of how the realizations respond to the different stress conditions are expected to be correct. In order to show how much anisotropy is expressed during the stimulations, box plots of the ratios comparing the three stimulation distances for each simulation are also presented.

The extents discussed in this paper include the full span of the affected fractures as shown in Figure 5, not just the distance from the injection point to their edge, so these distances are approximately double the radius of influence. Results from the different stress configurations are labeled using the convention "[Orientation]_[S_{Hmax}]_[S_{hmin}]" where "Rec" stands for the recommended values listed in Table 2, "Min" for minimum and "Max" for the maximum. For example, N25E_Rec_Rec is the label used for the most likely stress configuration.

3.1 Variation due to Stochastic Realizations of DFN

Figure 6 shows results for the most likely stress condition. One hundred DFN realizations were generated and then hydraulically fractured in FracMan. Figure 7 shows the same data in the more compact box plot format. Median values for each group are shown by the orange line. The 2nd and 3rd quartiles of the results are shown in the box portion while the whiskers extend to the max and min values.

The extent of the fractures that are inflated during the stimulation is approximately half that of those that experience shear failure. Note that the East-West extents are generally smaller than the North-South and Vertical extents which are very similar in size.

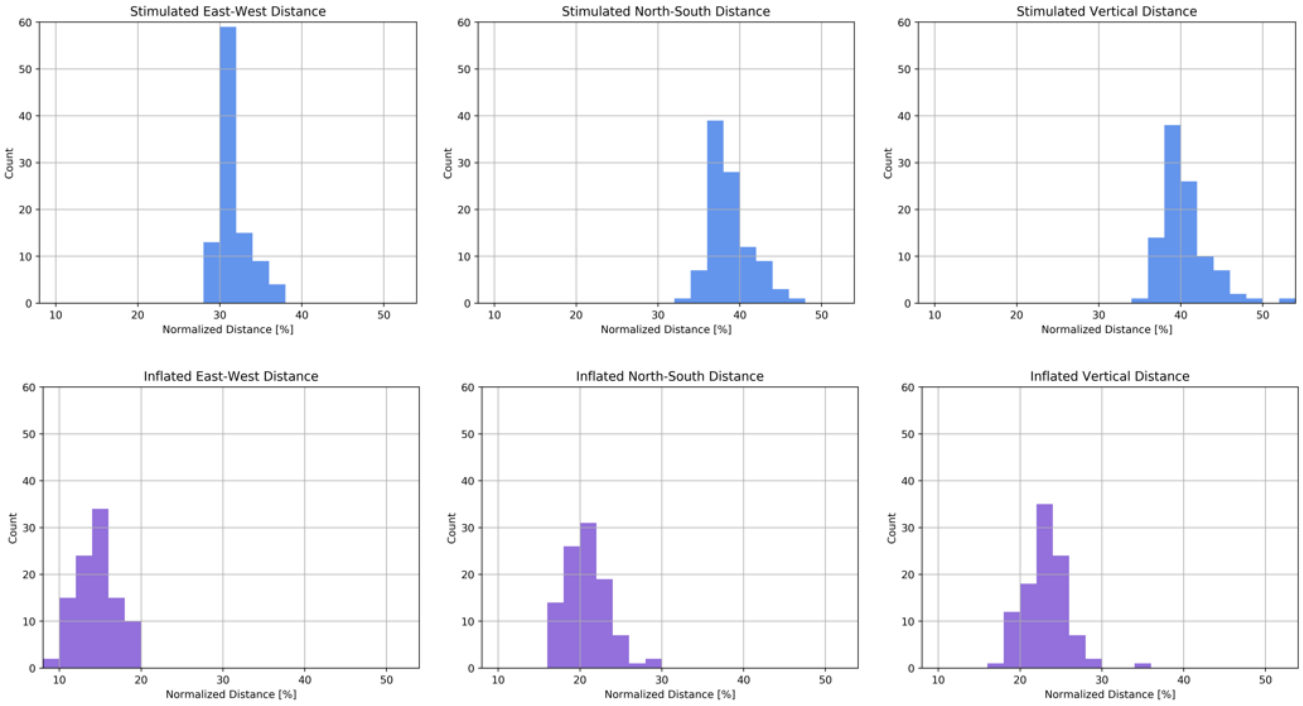

Figure 6: Histograms showing normalized hydraulic fracture stimulation extents for 100 DFN realizations under the most likely stress condition (N25E_Rec_Rec). The extent distances are shown as percentages of the hydraulic fracture region box size.

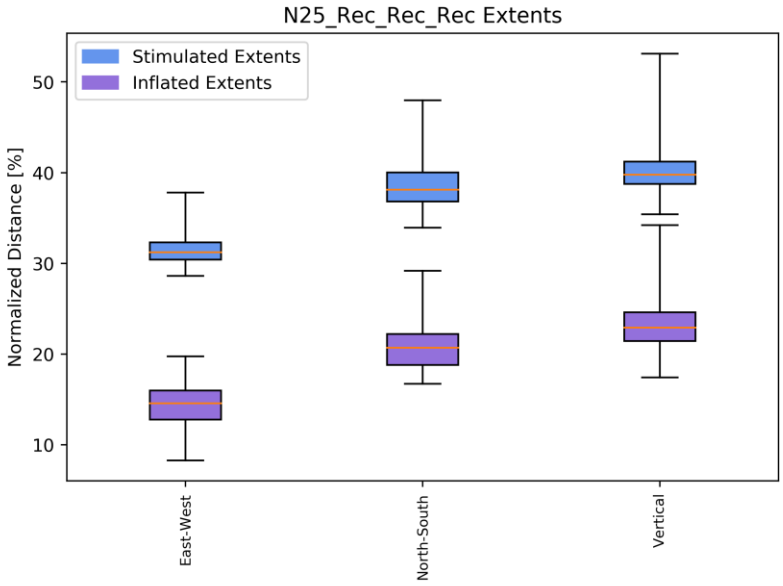

Figure 7: Box plots showing normalized hydraulic fracture stimulation distances for 100 DFN realizations under the most likely stress condition (N25E_Rec_Rec).

3.2 Variation due to Stress Conditions

The box plots shown in Figure 8 through Figure 11 show inflation and full stimulation extents for the 540 hydraulic simulations, grouped by the eighteen stress possible stress state combinations. Each stress condition includes the results from 30 DFN realizations. Note that each box plot figure is ordered by increasing median values, so the different stress states are potentially ordered differently for each plot.

The full stimulation region includes both the inflated fractures and those that experienced hydroshearing. Results for just the inflated fractures are shown separately. Stress conditions where the S_{hmin} gradient was equal to the recommended value are shown in green while those having the S_{hmin} gradient equal to the minimum value are shown in blue. The most likely stress condition is outlined with the grey box.

The choice to color the box plots based on the S_{hmin} gradient choice was made based on observations from Figure 8. The top plot showing the vertical extent of the stimulation is especially striking. The results for all of the stress conditions fall into two distinct populations; one group having shorter extents where the S_{hmin} gradient is set to the recommend value (shaded green) and another group having vertical extents almost twice as large where the S_{hmin} gradient is set to the minimum value (shaded blue). The spread in the vertical extent values between the two groups is larger than the spread due to the different DFN stochastic realizations as represented by the span of the box plot whiskers for each stress condition. These two groups are evident in the bottom plots of Figure 8 as well, which show the extents in the East-West and North-South dimensions, however the results are more mixed. Two of the stress combinations for the North_South extents having S_{hmin} equal to the recommended value plot with the larger extent stress combinations having S_{hmin} equal to the minimum value: N10E_Min_Rec and N25E_Min_Rec. The stress combination N25E_Min_Rec shows transitional behavior between the two groups for the East-West Extents. One additional stress combination, N40E_Min_Rec, also shows transitional behavior between the two groups for the North-South Extents. As with the vertical extents, the minimum S_{hmin} gradient group has East-West and North-South extents almost twice as large as the recommended S_{hmin} gradient group. Under the most likely stress conditions, N25E_Rec_Rec, the stimulated extents fall on the lower side of estimated values.

There are also patterns evident in Figure 8 in the variability due to the choice of stochastic DFN realization between both the two groups divided by the S_{hmin} gradient choice and the extent direction. In general, the minimum S_{hmin} gradient group shows higher inter-realization diversity compared with the recommended S_{hmin} gradient groups. The East-West extents show the lowest inter-realization diversity while the vertical extents show the highest inter-realization diversity. These difference might not be quite as large as they appear in the box plots if the range in values is normalized by the means, where, for example, a 50% variability would naturally appear as a larger span between the minimum and maximum values for a population having a higher mean compared with one with a lower mean.

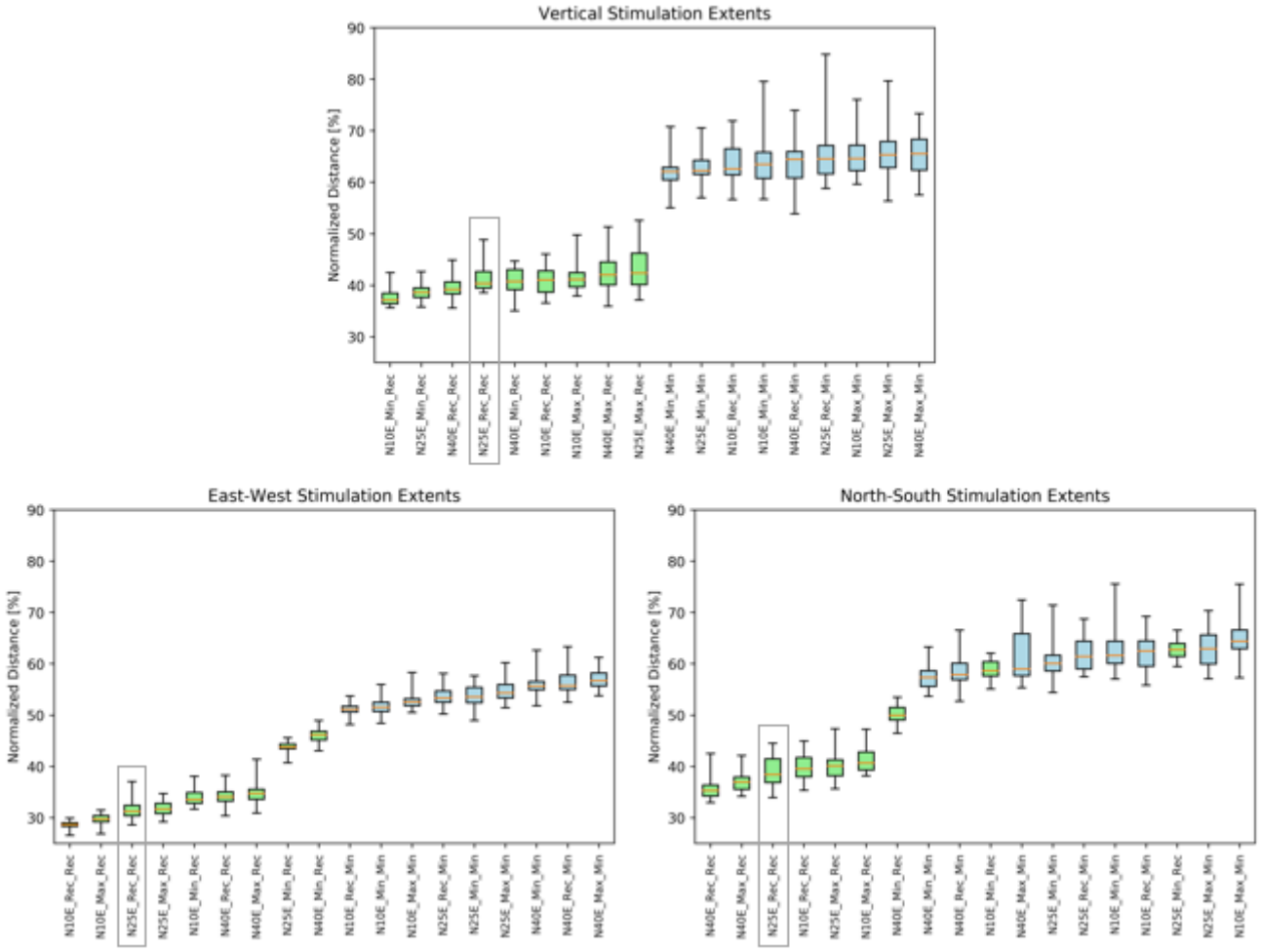

Figure 8: Stimulation extents of 540 hydraulic simulations, grouped by the 18 possible stress conditions.

Figure 9 shows the relationships between the different stimulation extent distances measured for each simulation. The East-West stimulation extents are always less than the North-South stimulation extents, with the ratio varying between 0.5 and slightly less than 1.0 as shown in the top plot. Stress conditions leading to the lower ratios result in more anisotropic stimulated volumes when viewed from above. This anisotropy seems to be mainly controlled by the orientation of S_{Hmax}: stress combinations including the N10E S_{Hmax} direction show the highest anisotropy while the stress combinations including the N40E S_{Hmax} direction show lowest anisotropy. This pattern is not evident in the lower two plots. In both these plots, the data can be divided into two groups, those stress conditions with ratios plotting below the 1.0 line where the lateral stimulation distance is less than the vertical stimulation distance, and those that plot above. The only three stress conditions that cause the lateral distance to exceed the vertical distance are N10E_Min_Rec, N25E_Min_Rec, and N40E_Min_Rec. For these stress conditions, it is not the S_{Hmax} orientation that controls this behavior, but the combination of experiencing the minimum S_{Hmax} gradient and the Recommended S_{hmin} gradient.

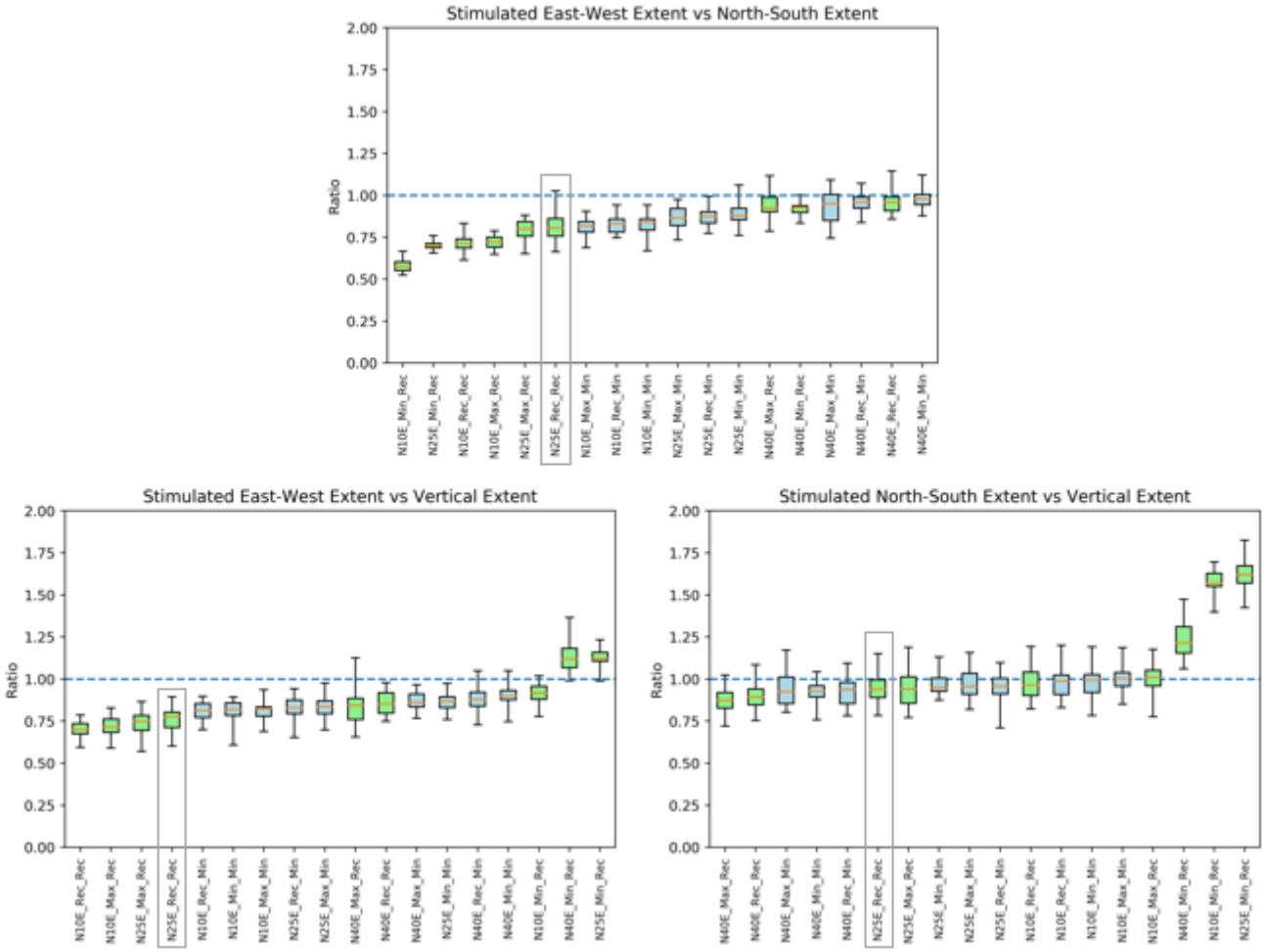

Figure 9: Ratios of stimulation extents of 540 hydraulic simulations, grouped by the 18 possible stress conditions.

The various directional extents of fractures inflated during hydraulic stimulation seem to be less affected by the choice of the evaluated stress conditions (Figure 10). The set of three stress conditions that showed lateral stimulation distances exceeding the vertical stimulation, N10E_Min_Rec, N25E_Min_Rec, and N40E_Min_Rec, also appear to have decreased vertical inflation extents (top plot in Figure 10). In general, the stress conditions having the minimum S_{hmin} gradient show more variability due to the choice of stochastic realization compared with those having the recommended S_{hmin} gradient. As with the full stimulation results, inflation distances in the East-West direction is less than inflation distances in the other two measured directions.

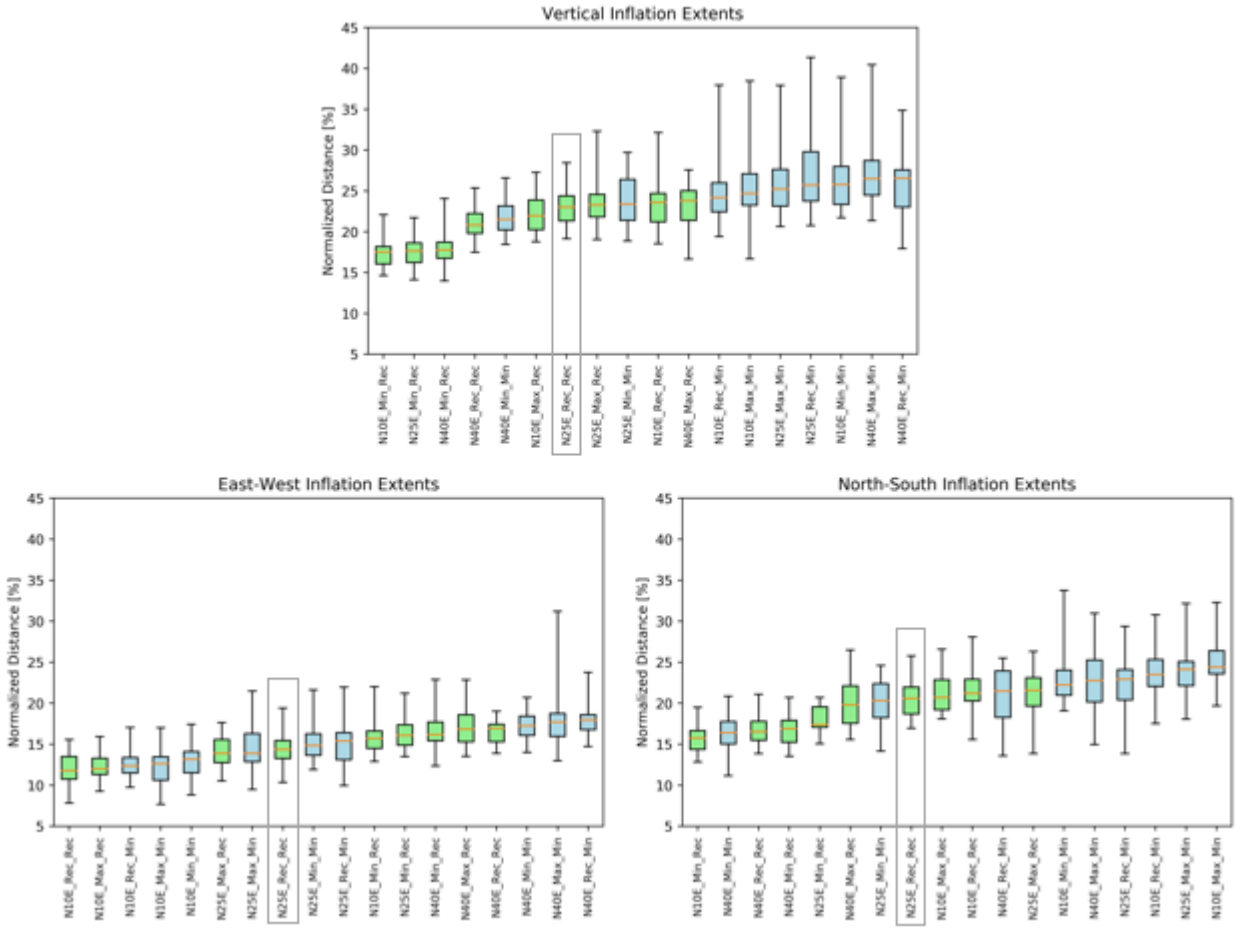

Figure 10: Inflation extents of 540 hydraulic simulations, grouped by the 18 possible stress conditions.

Figure 11 shows the relationships between the different inflated extent distances measured for each simulation. The ratio of inflated East-West extents vs inflated North-South extents appears to be significantly controlled by the direction of S_{Hmax} with a direction of N10E leading to the most anisotropy and the direction of N40E showing the least anisotropy, with notable exceptions for N10E_Min_Rec and N25E_Min_Rec. The ratio of inflated East-West extents vs inflated vertical extents follows the same pattern as for the East-West vs North-South extents, including the same exceptions. There does not appear to be a significant trend in the ratios of inflated North-South extents vs vertical extents.

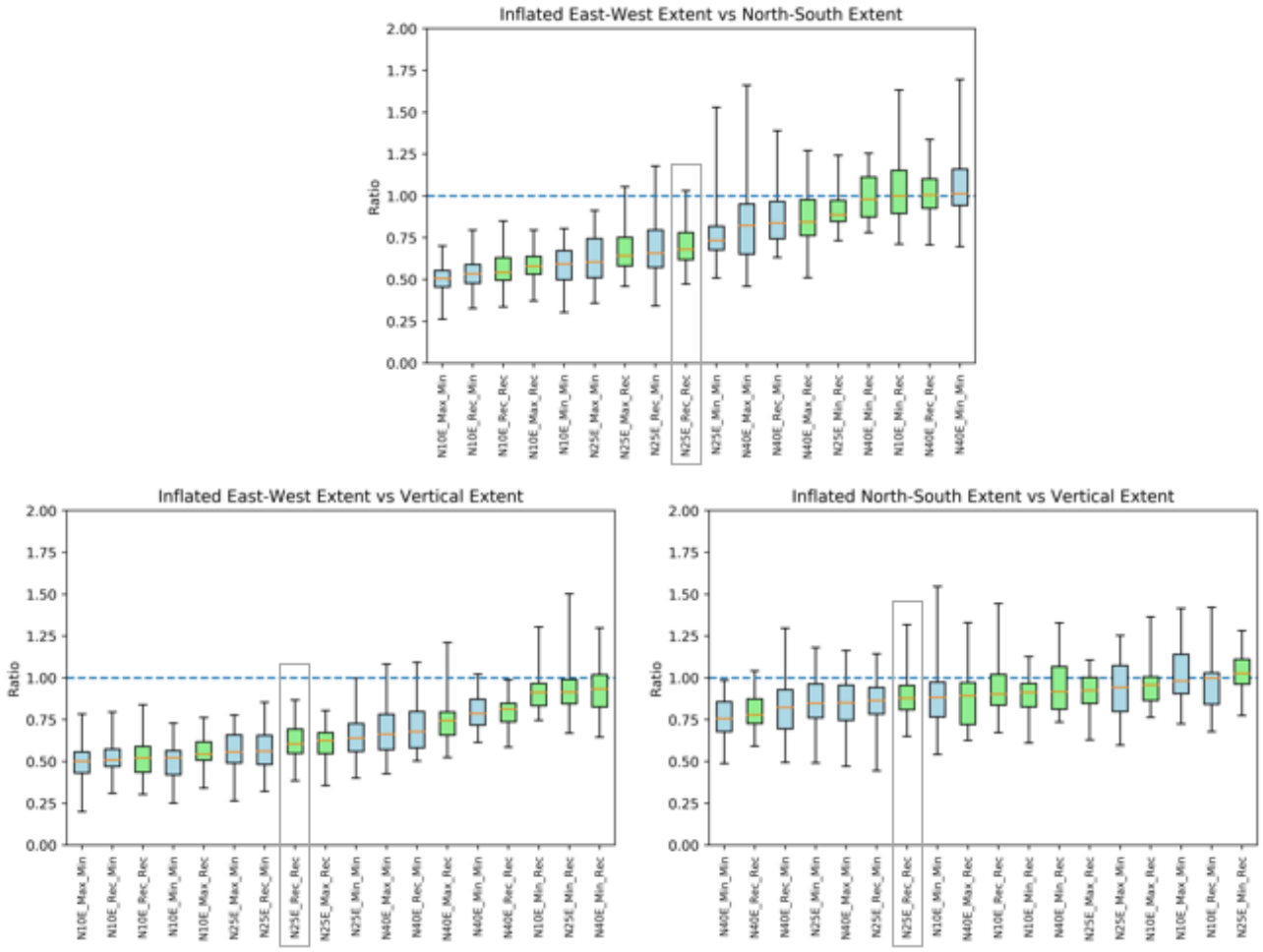

Figure 11: Ratios of inflation extents of 540 hydraulic simulations, grouped by the 18 possible stress conditions.

5. CONCLUSIONS

The current plan for the development of the FORGE site is to have a deep, inclined injection well and another inclined production well above it. Flow paths between the two are expected to be largely vertical in nature. Understanding the different patterns possible in the anisotropy of hydraulic stimulation due to a range of potential stress conditions is useful for planning simulation stage lengths for a given desired vertical distance. The variation due to the different S_{hmin} stress gradient end-members is very significant and introduces much more uncertainty in the stimulated extents compared to the variation due to the different stochastic realizations. This is apparent when including stimulation due to hydroshearing events vs just looking at inflation of natural fractures. Looking at the ratios comparing the extents, the stimulation in the East-West direction is consistently smaller than in the North-South or vertical directions. The North-South stimulation extent is very similar to the vertical extent except for the stress state combination using the minimum S_{Hmax} gradient and the recommend S_{hmin} gradient for the hydrosheared fractures where the North-South extent exceeds the vertical extent. This pattern is not evident when just looking at the more vertical inflated fractures.

Of more immediate utility, the identification of DFN realizations that exhibit average or end-member behavior is a prequel to sharing these realizations with other FORGE modeling team members having confidence in their applicability to the question at hand. For example, if the question being addressed is how much vertical extent would be expected during the hydraulic fracturing of the open hole

section of 16A(78)-32, Figure 12 and the summary statistics can show that the desired DFN realizations are N25E_Rec_Rec_20, N40E_Min_Rec_30, and N25E_Rec_Min_17. State-of-the-art, full physics simulations can then be employed on just these three fracture models to come up with predictions for the absolute stimulation distances expected during hydraulic stimulation.

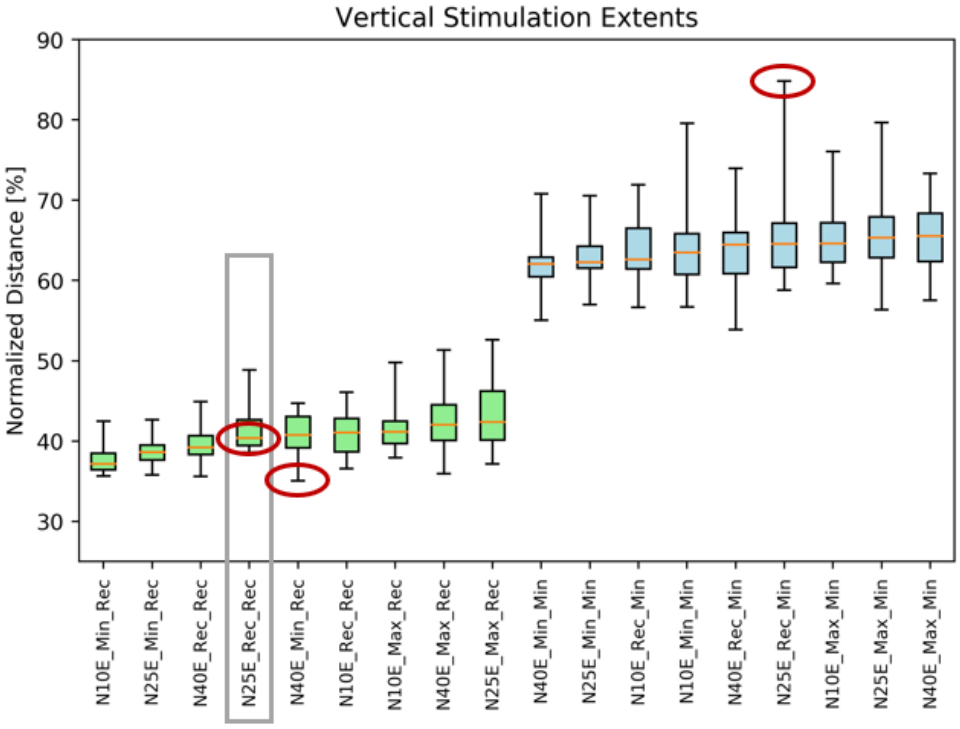

Figure 12: Vertical stimulation extents grouped by stress condition. The most likely stress condition is outlined in grey. Suggested average, minimum and maximum realizations for use in future simulation work are circled in red.

ACKNOWLEDGEMENTS

Funding for this work was provided by the U.S. DOE under grant DE-EE0007080 “Enhanced Geothermal System Concept Testing and Development at the Milford City, Utah FORGE Site”. We thank the many stakeholders who are supporting this project, including U.S. DOE Geothermal Technologies Office, Smithfield (Murphy Brown LLC), Utah School and Institutional Trust Lands Administration, and Beaver County as well as the Utah Governor’s Office of Energy Development.

REFERENCES

Cottrell M., Hosseinpour, H., and Dershowitz, W.: Rapid Discrete Fracture Analysis of Hydraulic Fracture Development in Naturally Fractured Reservoirs, Unconventional Resources Technology Conference, SPE-168843-MS, 13 p. (2013).

Dershowitz W., Ambrose, R., Lim, D., and Cottrell, M.: “Hydraulic Fracture and Natural Fracture Simulation for Improved Shale Gas Development,” American Association of Petroleum Geologists (AAPG) Annual Conference and Exhibition Houston (2011).

Finnila, A., Forbes, B., and Podgorney, R.: Building and Utilizing a Discrete Fracture Network Model of the FORGE Utah Site, *Proceedings,* 44th Workshop on Geothermal Reservoir Engineering, Stanford University, Stanford, CA (2019).

Golder Associates: FracMan® Reservoir Edition, version 7.9 Discrete Fracture Network Simulator (2020).

Moore, J. et al Energy and Geoscience Institute at the University of Utah: Utah FORGE: Phase 2C Topical Report, Section A. OVERVIEW of 2C Activities. Retrieved from https://gdr.openei.org/submissions/1187, (2019).

Simmons, S., Moore, J., Allis, R., Kirby, S., Jones, C., Bartley, J., Kleber, E., Knudsen, T., Miller, J., Hardwick, C., Rahilly, K., Gwynn, M., McLennan, J., Forbes, B., Podgorney, R., Pankow, K., Wannamaker, P., and Fischer, T.: A revised geoscientific model for FORGE Utah EGS Laboratory, *Proceedings,* 43rd Workshop on Geothermal Reservoir Engineering, Stanford University, Stanford, CA (2018).

Xing, P., Duane, W, Rickard, B., Barker, B., Finnila, A., Ghassemi, A., Pankow, K., Podgorney, R., Moore, J., Goncharov, A., McLennan, J.: Interpretation of In-Situ Injection Measurements at the FORGE Site, *Proceedings,* 45th Workshop on Geothermal Reservoir Engineering, Stanford University, Stanford, CA (2020).